Co-delivery of drugs and DNA from cationic core–shell nanoparticles self-assembled from a biodegradable copolymer

Wang, Yong; Gao, Shujun; Ye, Wen-Hui; Yoon, Ho Sup; Yang, Yi-Yan

2006

Wang, Y., Gao, S., Ye, W. H., Yoon, H. S., & Yang, Y. Y. (2006). Co-delivery of drugs and DNA from cationic core–shell nanoparticles self-assembled from a biodegradable copolymer. Nature Materials, 5(10), 791-796.

https://hdl.handle.net/10356/79958

https://doi.org/10.1038/nmat1737

Co-delivery of drugs and DNA from cationic core–shell nanoparticles self-assembled from a biodegradable copolymer

Yong Wang[1], Shujun Gao[1], Wen-Hui Ye[2], Ho Sup Yoon[2] &

*Yi-Yan Yang[1]**

[1]*Institute of Bioengineering and Nanotechnology, 31 Biopolis Way, The Nanos, Singapore 138669, Singapore*

[2]*School of Biological Sciences, Nanyang Technological University, 60 Nanyang Drive, Singapore 637551, Singapore*

**e-mail: yyyang@ibn.a-star.edu.sg*

Non-viral gene-delivery systems are safer to use and easier to produce than viral vectors, but their comparatively low transfection efficiency has limited their applications[1]. Co-delivery of drugs and DNA has been proposed to enhance gene expression or to achieve the synergistic/combined effect of drug and gene therapies[2–6]. Attempts have been made to deliver drugs and DNA simultaneously using liposomes[7]. Here we report cationic core–shell nanoparticles that were self-assembled from a biodegradable amphiphilic copolymer. These nanoparticles offer advantages over liposomes, as they are easier to fabricate, and are more readily subject to modulation of their size and degree of positive charge. More importantly, they achieve high gene-transfection efficiency and the possibility of co-delivering drugs and genes to the same cells. Enhanced gene transfection with the co-delivery of paclitaxel has been demonstrated by *in vitro* and *in vivo* studies. In particular, the co-delivery of paclitaxel with an interleukin-12-encoded plasmid using these nanoparticles suppressed cancer growth more efficiently than the delivery of either paclitaxel or the plasmid in a 4T1 mouse breast cancer model. Moreover, the co-

delivery of paclitaxel with Bcl-2-targeted small interfering RNA (siRNA) increased cytotoxicity in MDA-MB-231 human breast cancer cells.

In this study, we have designed a biodegradable cationic amphiphilic copolymer, which consists of cholesterol side chains and a cationic main chain. This polymer can easily form core–shell nanoparticles with a hydrophobic cholesterol core and a cationic shell in an aqueous solution by a self-assembly process. Hydrophobic drugs can be incorporated into the core during the self-assembly process. The cationic shell of the resulting drug-loaded nanoparticles can be used to bind DNA.

The cationic amphiphilic polymer was derived by a three-step synthesis (Fig. 1). First, the main chain, poly(*N*-methyldietheneamine sebacate) (PMDS), was produced by condensation polymerization between *N*-methyldiethanolamine and sebacoyl chloride. Excess triethylamine was used to remove hydrochloride and limit protonation of the tertiary amine. Next, cholesteryl chloroformate was allowed to react with 2-bromoethylamine hydrobromide in an amidation reaction. The resulting hydrophobic *N*-(2-bromoethyl) carbarmoyl cholesterol was then grafted onto the hydrophilic PMDS main chain through a quaternization reaction to obtain the cationic amphiphilic copolymer, poly{(*N*-methyldietheneamine sebacate)-*co*-[(cholesteryl oxocarbonylamido ethyl) methyl bis(ethylene) ammonium bromide] sebacate} (P(MDS-*co*-CES)). The product was characterized by ^{1}H nuclear magnetic resonance and infrared spectroscopies (see Supplementary Information, Figs S1–S6). The main chain was a polyester, and the pendant chain contained potentially hydrolytically labile urethano groups, rendering this copolymer degradable. The degree of cholesterol grafting was ~30−40%. P(MDS-*co*-CES) had a weight-average molecular mass of 9.1 kilodaltons with a polydispersity of 2.0, as measured by gel permeation chromatography. Its critical association concentration in water was determined to be 1.9 mgl^{-1} (see Supplementary Information, Fig. S7).

Like other amphiphilic copolymers[8], P(MDS-*co*-CES) could self-assemble in an aqueous solution to form core–shell nanoparticles. 15.0mg of polymer was dissolved in 5.0 ml of dimethylformamide, and dialysed against 500 ml of deionized water and sodium acetate/acetic acid buffers (pH = 5.6 and 4.6). The resulting core–shell nanoparticles were characterized by a zeta-potential analyser with dynamic light-

scattering capability (ZetaPlus). Their effective diameters in deionized water and sodium acetate/acetic acid buffers were 160, 96 and 82 nm with polydispersity indices of 0.15, 0.24 and 0.24, respectively. The respective zeta potentials of the nanoparticles were 44±2, 72±2 and 84±5 mV. At a lower pH, the nanoparticles possessed a higher zeta potential due to protonation of the tertiary amine on the polymer main chain. The surface charge of the nanoparticles can also be manipulated by varying the degree of cholesterol grafting.

To evaluate the possibility of using this copolymer to co-deliver a drug and DNA, paclitaxel, indomethacin and pyrene were encapsulated as model drugs first in the core–shell nanoparticles by the membrane dialysis method. The encapsulation efficiencies of paclitaxel, indomethacin and pyrene were determined by ultraviolet spectroscopy to be 91.7%, 78.4% and 55.6%, respectively. The polymer particle size increased from 83 ± 1 to 119 ± 3, 175 ± 2 and 180 ± 2 nm after loading with paclitaxel, indomethacin and pyrene, respectively. The drug-loading efficiency of the nanoparticles highly depended on the compatibility of the drug and the core-forming segments[9]. The nanoparticles showed lower encapsulation efficiency for pyrene, possibly because of pyrene's rigid structure being less compatible with the polymer's cholesteryl moieties. The zeta potential of the nanoparticles decreased from 84±5 to 68±3, 63±2 and 65±1 mV, respectively, after paclitaxel, indomethacin and pyrene encapsulation.

Next, plasmid DNA encoding the 6.4kb firefly luciferase (pCMV-luciferase VR1255_C) driven by the cytomegalovirus promoter (Carl Wheeler) was bound to the blank core–shell nanoparticles, and paclitaxel-, indomethacin- and pyrene-loaded core–shell nanoparticles in the sodium acetate buffer (0.02 M, pH 4.6). Plasmid DNA complexed with the core–shell nanoparticles exhibited decreased mobility in an electromobility shift assay (Fig. 2a). Complete retardation of the DNA was achieved at an *N/P* ratio (molar ratio of nitrogen atom content in the polymer to phosphorous atom content in the DNA) of 2, 3, 3 and 3 for blank core–shell nanoparticles, and paclitaxel-, indomethacin- and pyrene-loaded core–shell nanoparticles, respectively. The DNA-binding ability of the blank core–shell nanoparticles was slightly greater than that of the drug-loaded core–shell nanoparticles due to the greater zeta potential of the former.

To determine the structural integrity of the drug-loaded core–shell nanoparticles during the DNA binding process, the microenvironment of the pyrene-loaded nanoparticles was studied with an LS50B luminescence spectrometer (Perkin Elmer) at room temperature. The ratios of the peak intensities at 338 and 333 nm (*I*338/*I*333) of the excitation spectra of various samples are presented in Fig. 2b. A higher ratio would be expected when pyrene was located in a more hydrophobic environment[10]. Indeed, the *I*338/*I*333 ratio increased when pyrene was loaded into the core–shell nanoparticles. Interestingly, the DNA binding further improved the hydrophobicity of pyrene's microenvironment, indicating that pyrene remained in the core of the nanoparticles after DNA binding. The size of pyrene-loaded core–shell nanoparticle/DNA complexes ranged from 140 to 300 nm for *N/P* ratios of 0.2–25 (see Supplementary Information, Fig. S8), indicating that pyrene-loaded nanoparticles did not collapse during DNA binding. These findings demonstrated the ability of the core–shell nanoparticles to carry a drug and DNA simultaneously in a stable colloid. Indomethacin release rates from indomethacin-loaded nanoparticles and indomethacin-loaded nanoparticle/DNA complexes were similar, indicating that DNA binding did not affect its release rate significantly (see Supplementary Information, Fig. S9). However, paclitaxel release from the nanoparticles was slightly faster than that from the nanoparticle/DNA complexes, but slower than indomethacin due to its greater hydrophobicity (see Supplementary Information, Fig. S10).

To evaluate the potential application of these nanoparticles for gene delivery, *in vitro* transfection experiments were conducted on human embryonic kidney (HEK293) mammalian cell line, HepG2 cell line and 4T1 mouse breast cancer cell line (ATCC) using the GFP reporter gene encoding the GFPmut1 variant (pEGFP-C1) with 4.7kb driven by the SV40 early promoter (Clontech) and the luciferase reporter gene. The nanoparticle/DNA complexes were incubated with the cells for 4 h. As with polyethylenimine (PEI, branched and molecular mass = 25,000), the gene transfection efficiency depended strongly on the cell type and the *N/P* ratio of the nanoparticles. It is expected that this polymer would provide high gene transfection efficiency as its main chain was designed with both a quaternary ammonium group (for DNA binding) and a tertiary amine group (for endosomal buffering[11]). As shown in Fig. 3a,b, the

nanoparticle/DNA complexes yielded the highest GFP and luciferase transfection efficiency in HEK293 cells at an *N/P* ratio of 15, which was comparable to that of PEI. In HepG2 cells, the highest luciferase expression was also achieved at an *N/P* ratio of 15, which was slightly lower than that of PEI (Fig. 3d). However, the GFP expression was much higher for the nanoparticles than for PEI (Fig. 3c). A higher GFP expression level indicates that the percentage of cells transfected with the GFP gene was higher. The uptake of the nanoparticle/DNA complexes by HepG2 cells might be higher than that of PEI/DNA complexes, possibly due to the highly positive charge of the complexes (see Supplementary Information, Fig. S8), leading to greater GFP expression. However, the intracellular delivery of DNA by the nanoparticles might be less effective in HepG2 cells when compared with PEI, resulting in a slightly lower overall gene expression level (that is, the luciferase expression level). In 4T1 cells, the nanoparticle/DNA complexes provided greater GFP and luciferase expressions, compared with PEI (Fig. 4a,b). In addition, we have also demonstrated that these nanoparticles were able to transfect small interfering RNA (siRNA) silencing the anti-apoptotic protein Bcl-2, in which the target sequence was chemically synthesized with 3'-dTdT overhang (GUA CAU CCA UUA UAA GCU G dTdT, Dharmacon RNA Technologies). The nanoparticle/siRNA complexes down-regulated Bcl-2 expression in MDA-MB-231 human breast cancer cells (see Supplementary Information, Fig. S11). We noted that the amount of nanoparticles used for the optimal complexes was significantly lower than their IC50 values. The IC50 values of the nanoparticles were determined by 3-(4,5-dimethylthiazol-2-yl)-2,5-diphenyl tetrazolium bromide (MTT) assay to be 166, 129 and 189 g ml^{-1} for HEK293, HepG2 and 4T1 cells, respectively, which were higher than those of PEI (16, 18 and 22 g ml^{-1}, respectively) (see Supplementary Information, Fig. S12). It is hypothesized that the cytotoxicity of cationic polymers or nanoparticles was caused by electrostatic interactions with negatively charged glycocalyx of the cell surface[12]. The nanoparticle/DNA complexes exhibited lower cytotoxicity than the nanoparticles, possibly due to the reduced surface charge (see Supplementary Information, Fig. S12c). The nanoparticles had hydrophobic cores of cholesterol moieties, more suitable for the incorporation of hydrophobic drugs than hydrophilic drugs. As most anticancer drugs are hydrophobic,

these nanoparticles would have a great potential for co-delivering anticancer drugs and genes for improved cancer therapy.

To illustrate the advantage of co-delivery of a drug and gene, paclitaxel-loaded nanoparticles were used to deliver the luciferase and GFP reporter genes. It was expected that the presence of paclitaxel would enhance gene expression possibly because of its anti-mitotic function[13,14]. In the course of an *in vitro* study, it might be acceptable to pretreat the cells with paclitaxel before transfection. However, for *in vivo* applications, it would be more advantageous to transport the drug with DNA in the same carrier so that both the drug and DNA could be delivered to the same cells for combined actions and synergistic effects. As shown in Fig. 4b, the co-encapsulated paclitaxel did give rise to an ~11-fold increase in luciferase level at an *N/P* ratio of 15, similar to the formulation of nanoparticle/DNA complexes plus paclitaxel dissolved in dimethyl sulphoxide (DMSO). However, the pretreatment of cells with paclitaxel-loaded nanoparticles did not improve the luciferase expression level, probably because paclitaxel and DNA were not delivered to the same cells by the separate formulations. The co-encapsulated paclitaxel also led to an increased GFP expression (by ~8-fold) at an *N/P* ratio of 15 (Fig. 4a). *In vivo* transfection experiments were carried out on mice bearing subcutaneous 4T1 breast tumours using the luciferase reporter gene. The blank and paclitaxel-loaded nanoparticles, as well as PEI/DNA complexes, were administered locally at the tumour sites. After two days, the highest luciferase activity induced in tumours by the nanoparticles (*N/P* ratio = 25) was greater than that induced by PEI (see Supplementary Information, Fig. S13). The co-delivery of paclitaxel further enhanced luciferase activity by seven times at the same *N/P* ratio. We note that paclitaxel-loaded nanoparticles were slightly more toxic to 4T1 cells than the pure nanoparticles, but the amount of paclitaxel-loaded nanoparticles used for *in vitro* and *in vivo* transfection studies was lower than their IC50 value (see Supplementary Information, Fig. S14). To further demonstrate the synergistic/combined effect of co-delivery of a therapeutic drug and gene *in vivo*, interleukin-12 (IL-12)-encoded plasmid was used as a therapeutic gene to be co-delivered with paclitaxel into the 4T1 mouse breast tumours, which share many characteristics with human breast tumours[6], by local injection. IL-12 is a highly potent anti-tumour cytokine, and may also overcome paclitaxel-mediated T-cell suppression. As shown in Fig. 4c, the

tumour growth rate in the mice treated with paclitaxel-loaded nanoparticle/IL-12-encoded plasmid complexes was significantly lower than that in the mice treated with either paclitaxel-loaded nanoparticles or nanoparticle/IL-12 gene complexes ($P < 0.001$), suggesting a significant synergistic/combined effect of co-delivery of paclitaxel and the IL-12 gene. Similar phenomena were reported using two separate injections, that is, the IL-12 gene transfected by PEI-*g*-cholesterol through local injection at the tumour sites and paclitaxel delivered by another polymer carrier, HySolv via the tail vein[6]. Clearly, by using the nanoparticles developed in this study, which carry the drug and gene simultaneously, the number of injections and the amount of the drug and gene can be reduced significantly, yet a synergistic/combined effect can be achieved.

The plasmids could be replaced with synthetic siRNA molecules. Here, to test this hypothesis, paclitaxel and Bcl-2-targeted siRNA were used as a pair to demonstrate the synergistic effect of drug and gene delivery in the same vehicle. MDA-MB-231 cells were first incubated with the nanoparticle/siRNA complexes for 4h. After 24h, the cells were treated for 48 h with paclitaxel-loaded nanoparticle/siRNA complexes containing 20 nM of siRNA. The cell viability decreased from 78% to 59% and from 58% to 39% in the presence of the siRNA at paclitaxel concentrations of 100 and 400 nM, respectively (Fig. 4d). As the cytotoxicity of the siRNA was only ~8%, there was indeed a synergistic effect associated with the co-delivery of paclitaxel and siRNA, possibly because the suppression of the anti-apoptotic activity of Bcl-2 by the siRNA made the cells more sensitive to paclitaxel.

METHODS

SYNTHESIS OF P(MDS-*co*-CES)

Synthesis of PMDS: 5.958 g of *N*-methyldiethanolamine (0.05 mol) and 50.5 g of triethylamine (0.5 mol) were added to a 150 ml round-bottom flask in a dry ice/acetone bath (below −30 °C). 40 ml of tetrahydrofuran (dried with sodium) containing 11.945 g of sebacoyl chloride (0.05 mol) were added dropwise to the flask with stirring. The flask was removed 1 h later, and the reaction was allowed to proceed at room temperature overnight. The solvent and residual triethylamine were removed using a Rotavapor. The

crude product dissolved in 100 ml of toluene was extracted four times with 50 ml of NaCl-saturated aqueous solution, and then dialysed in acetone using a membrane with a molecular mass cutoff of 3.5 kdaltons. Acetone was subsequently removed from the dialysate using the rotavapor, and the final product was dried in a vacuum oven for 2 days. The yield was ~75%.

Synthesis of *N*-(2-bromoethyl) carbarmoyl cholesterol: 50 ml of chloroform dried with a molecular sieve was put into a 100 ml round-bottom flask in a dry ice/acetone bath. 4.34 g of cholesteryl chloroformate (0.0097 mol) and 2.18 g of 2-bromoethylamine hydrobromide (0.0106mol) were then added with stirring. Next, 3 ml of freshly dried triethylamine were added to the flask, which was moved after 30 min for the reaction to proceed at room temperature for 12 h. The organic solution was washed 3 times with 20 ml of 1 N HCl solution saturated with NaCl, and once with 30 ml of NaCl-saturated aqueous solution to remove residual triethylamine. The organic phase was collected and dried with 5 g of anhydrous magnesium sulphate. The solution was then filtered and distilled. The crude product was recrystallized with anhydrous ethanol once, and with anhydrous acetone twice. The final product was dried with a vacuum oven for 24 h. The yield was ~78%.

Synthesis of P(MDS-*co*-CES): 2.85 g of PMDS (0.01 mol) and 5.5 g of *N*-(2-bromoethyl) carbarmoyl cholesterol (0.01 mol) were dissolved in 50ml of dry toluene, and refluxed for 2 days under argon. 250 ml of diethyl ether was then added to precipitate the product. To completely remove unreacted *N*-(2-bromoethyl) carbarmoyl cholesterol, the product was washed with diethyl ether 4 more times. The yield was ~70%.

TRANSFECTION STUDIES

HEK293, HepG2 and MDA-MB-231 cells were maintained in Dulbecco's modified Eagle's medium (DMEM), and 4T1 cells were maintained in RPMI 1640 at 37°C under an atmosphere with 5% CO_2. Both DMEM and RPMI 1640 were supplemented with 10% fetal bovine serum, 2mM L-glutamine, 100 Uml^{-1} penicillin and 100 μgml^{-1} streptomycin. Cells were seeded onto 24-well plates at a density of 8×10^4 cells per well for luciferase gene transfection, and 12-well plates at a density of 2×10^5 cells per well for

GFP gene transfection, and cultivated in 0.5 ml and 1.0 ml of growth medium respectively. After 24 h, complexes containing 2.5 μg of luciferase-encoded plasmids or 3.5 μg of GFP-encoded plasmids were added to each well. After 4 h of incubation, the culture media were replaced with fresh ones. The culture media were removed after two days, and the cells on the 24-well plates were washed with 0.5 ml of phosphate-buffered saline (PBS). 0.2 ml of reporter lysis buffer was then added to each well to lyse the cells. Next, the cell suspension was frozen to −80°C for 30 min and thawed, followed by centrifugation at 14,000 r.p.m. for 5 min. The relative light units (RLU) were measured using a luminometer (Bio-Rad), and normalized to the protein content using the bicinchoninic acid (BCA) protein assay (Bio-Rad). For the GFP gene transfection, the cells were harvested by a different protocol: after 2 days of incubation, the cells on the 12-well plates were washed with 1.0 ml of PBS. 0.3 ml of 1×trypsin solution was then added to each well, which was incubated at room temperature for 10–15 min to detach the cells. The cell suspension was centrifuged at 14,000 r.p.m. for 5 min, and re-suspended in PBS (pH 7.4). On separation from PBS by centrifugation, the cells were suspended in 0.3 ml of 1% paraformaldehyde for fixation before analyses by a cell cytometer (EPICS ELITE ESP, Coulter). The experimental details for siRNA transfection in MDA-MB-231 cells are described in Supplementary Information.

For *in vivo* luciferase transfection experiments, female Balb/c mice (Laboratory Animals Center, Singapore) weighing 20–30 g were injected with 200 μl of a cell suspension containing 1×10^6 4T1 cells subcutaneously. After 2–3 weeks, when the tumour reached ~4−6 mm in diameter, 30 μl of the nanoparticles or PEI/DNA complexes containing 2.0 μg of luciferase-encoded plasmid were injected into the tumour of each mouse. The tumour tissues were harvested, homogenized and analysed for luciferase activity at 48 h. Each RLU reading was obtained from 8 animals, and expressed as an average value. The 4T1 tumour-bearing mice (n = 5) without treatment were used as the control. The RLU readings in the tumours of the control group were subtracted from those of the mice treated with the complexes.

For *in vivo* co-delivery of the IL-12 gene and paclitaxel, the same animal model was used. The doses of IL-12 and paclitaxel used were 5 and 10 μg per mouse respectively.

The complexes were formed at an *N/P* ratio of 10. The size of the tumours was measured immediately before each treatment using electronic digital Vernier calipers along the longest width (*W*) and the corresponding perpendicular length (*L*), and the tumour volume (Lx $(0.5W)^2$) was calculated. The tumour growth rate was calculated based on the formula: {[volume of the tumour at the point of measurement (V_t) −volume of the tumour on the first day of treatment (V_0)]/V_0}x100%.

Acknowledgements

The authors thank K. W. Leong (Johns Hopkins School of Medicine), J. Y. Ying (Institute of Bioengineering and Nanotechnology (IBN)), S. Wang (IBN), X.-G. Wang (Tsinghua University, P. R. China) and S. H. Goh (National University of Singapore) for valuable discussions. They acknowledge the technical assistance and contribution of X. Jiang (Johns Hopkins Singapore), C.-W. Tan, R. Ruan and K.-H. Foong (IBN). This work was funded by the IBN (Agency for Science, Technology and Research, Singapore).

Correspondence and requests for materials should be addressed to Y.-Y.Y.

Author contributions

Y.W. was responsible for polymer synthesis and *in vitro* experiments, and worked on animal experiments together with S.G. W.-H.Y. and H.S.Y. were responsible for siRNA experiments. Y.-Y.Y. was in charge of polymer design, project initiation, project planning and overseeing the project.

Competing financial interests

The authors declare that they have no competing financial interests.

References

1. Luo, D. & Saltzman, W. M. Synthetic DNA delivery systems. *Nature Biotechnol.* **18,** 33–37 (2000).

2. Zhang, X. H. *et al*. *In vivo* gene delivery via portal vein and bile duct to individual lobes of the rat liver using a polylysine-based nonviral DNA vector in combination with chloroquine. *Human Gene Therapy* **12,** 2179–2190 (2001).

3. Cotten, M. *etal*. High-efficiency receptor-mediated delivery of small and large (48kb) gene constructs using the endosome disruption activity of defective or chemically inactivated adenovirus particles. *Proc. Natl Acad. Sci. USA* **89,** 6094–6098 (1992).

4. Malone, R. W. *et al*. Dexamethasone enhancement of gene expression after direct hepatic DNA injection. *J. Biol. Chem.* **269,** 29903–29907 (1994).

5. Kishida, T. *et al*. Electrochemo-gene therapy of cancer: intratumoral delivery of interleukin-12 gene and bleomycin synergistically induced therapeutic immunity and suppressed subcutaneous and metastatic melanomas in mice. *Molecular Therapy* **8,** 738–745 (2003).

6. Jan´at-Amsbury, M. M. *et al*. Combination of local, nonviral *IL12* gene therapy and systemic paclitaxel treatment in a metastatic breast cancer model. *Molecular Therapy* **9,** 829–836 (2004).

7. Liu, F., Shollenberger, L. M. & Huang, L. Non-immunostimulatory nonviral vectors. *FASEB J.* **18,** 1779–1781 (2004).

8. Kataoka, K., Harada, A. & Nagasaki, Y. Block copolymer micelles for drug delivery: Design, characterization and biological significance. *Adv. Drug Delivery Rev.* **47,** 113–131 (2001).

9. Allen, C., Maysinger, D. & Eisenberg, A. Nano-engineering block copolymer aggregates for drug delivery. *Colloids Surf. B* **16,** 3–27 (1999).

10. Dong, D. C. & Winnik, M. A. The Py scale of solvent polarities. *Can. J. Chem.* **62,** 2560–2565 (1984).

11. Wood, K. C., Little, S. R., Langer, R. & Hammond, P. T. A family of hierarchically self-assembling linear hybrid polymers for highly efficient targeted gene delivery. *Angew. Chem. Int. Edn* **44,** 2–7 (2005).

12. Fischer, D., Li, Y., Ahlemeyer, B., Krieglstein, J. & Kissel, T. *In vitro* cytotoxicity testing of polycations: influence of polymer structure on cell viability and hemolysis. *Biomaterials* **24,** 1121–1131 (2003).

13. Son, K. & Huang, L. Factors influencing the drug sensitization of human tumor cells for *in situ* lipofection. *Gene Therapy* **3,** 630–634 (1996).

14. Nair, R. R., Rodgers, J. R. & Schwarz, L. A. Enhancement of transgene expression by combining glucocorticoids and anti-mitotic agents during transient transfection using DNA-cationic liposomes. *Molecular Therapy* **5,** 455–462 (2002).

List of Figures

expressed as an average value). **d**, Viability of MDA-MB-231 cells against (1) the nanoparticles, (2) nanoparticle/siRNA complexes, (3,5) paclitaxel-loaded nanoparticles and (4,6) paclitaxel-loaded nanoparticle/siRNA complexes. The paclitaxel concentrations were (3,4) 100 nM and (5,6) 400 nM. The standard deviation is shown by the error bars.

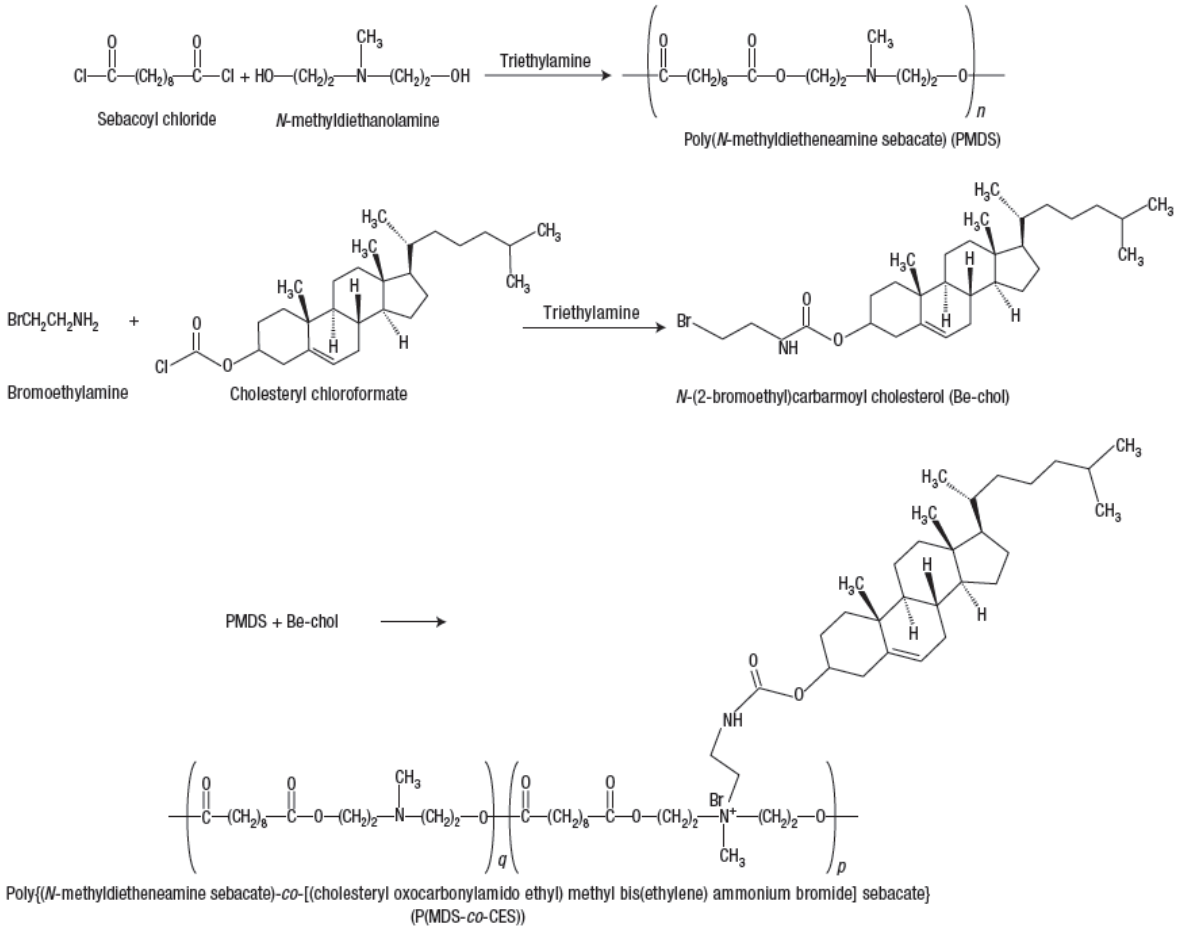
Triethylamine
Sebacoyl chloride
N-methyldiethanolamine
Poly(N-methyldietheneamine sebacate) (PMDS)
BrCH2CH2NH2
Bromoethylamine
Cholesteryl chloroformate
Triethylamine
N-(2-bromoethyl)carbarmoyl cholesterol (Be-chol)
PMDS + Be-chol
Poly{(N-methyldietheneamine sebacate)-co-[(cholesteryl oxocarbonylamido ethyl) methyl bis(ethylene) ammonium bromide] sebacate}
(P(MDS-co-CES))

Figure 1

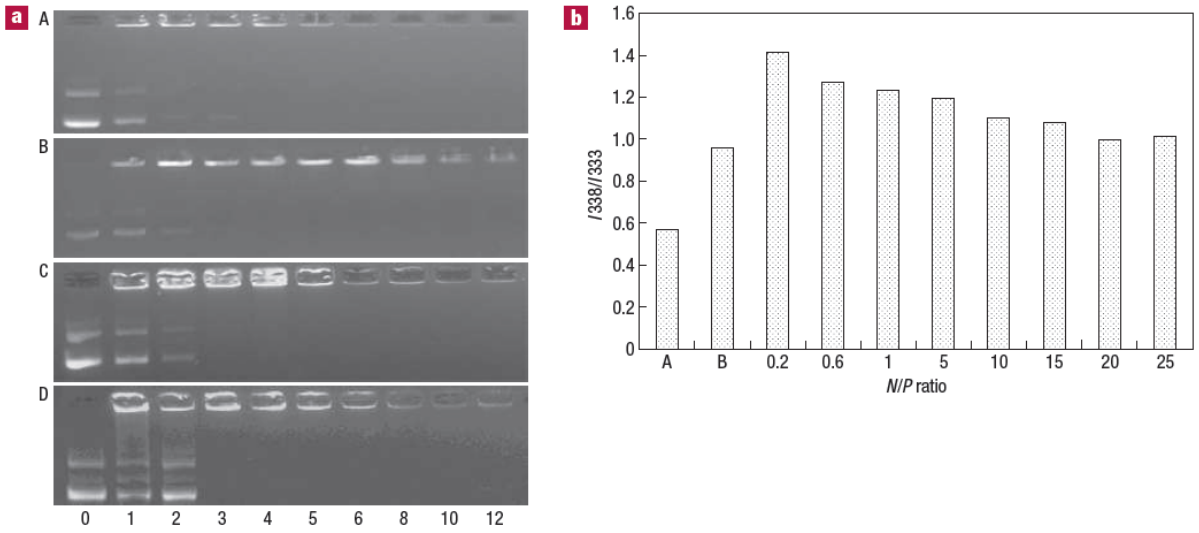
a
A
B
C
D
0 1 2 3 4 5 6 8 10 12
b
I338/I333
1.6
1.4
1.2
1.0
0.8
0.6
0.4
0.2
0
A B 0.2 0.6 1 5 10 15 20 25
N/P ratio

Figure 2

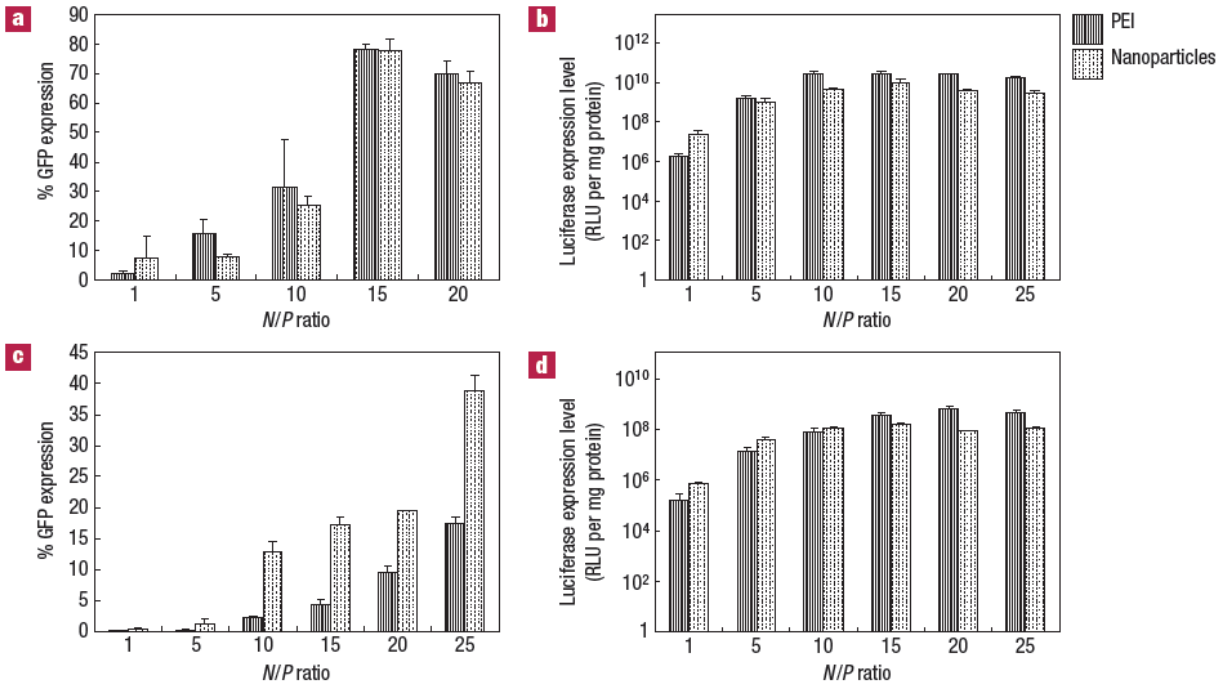
a
% GFP expression
N/P ratio
b
Luciferase expression level (RLU per mg protein)
N/P ratio
PEI
Nanoparticles
c
% GFP expression
N/P ratio
d
Luciferase expression level (RLU per mg protein)
N/P ratio

Figure 3

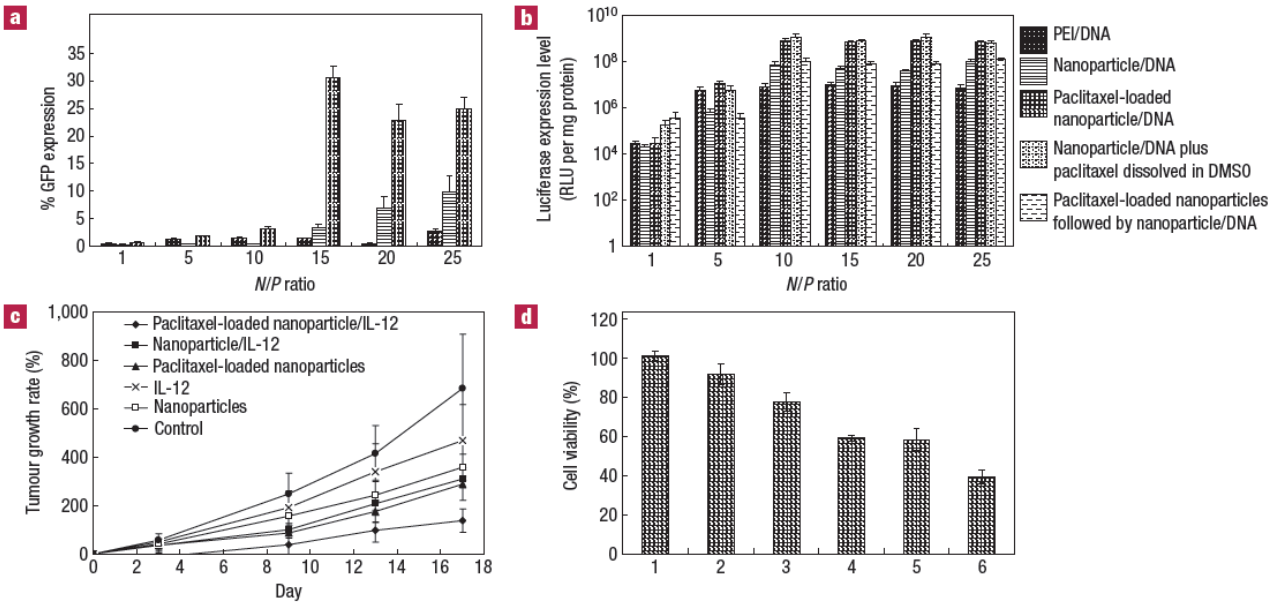
a
% GFP expression
N/P ratio
b
Luciferase expression level (RLU per mg protein)
N/P ratio
PEI/DNA
Nanoparticle/DNA
Paclitaxel-loaded nanoparticle/DNA
Nanoparticle/DNA plus paclitaxel dissolved in DMSO
Paclitaxel-loaded nanoparticles followed by nanoparticle/DNA
c
Tumour growth rate (%)
Day
Paclitaxel-loaded nanoparticle/IL-12
Nanoparticle/IL-12
Paclitaxel-loaded nanoparticles
IL-12
Nanoparticles
Control
d
Cell viability (%)

Figure 4